# Enhanced hysteresis in the semiconductor-to-metal phase transition of $VO_2$ precipitates formed in $SiO_2$ by ion implantation

R. Lopez,[a] L. A. Boatner, and T. E. Haynes
*Solid State Division, Oak Ridge National Laboratory, Oak Ridge, Tennessee 37831*

R. F. Haglund, Jr., and L. C. Feldman[b]
*Department of Physics and Astronomy, Vanderbilt University, Nashville, Tennessee 37235*

(Received 19 June 2001; accepted for publication 27 August 2001)

A strongly enhanced hysteresis with a width of $>34\,^{\circ}C$ has been observed in the semiconductor-to-metal phase transition of submicron-scale $VO_2$ precipitates formed in the near-surface region of amorphous $SiO_2$ by the stoichiometric coimplantation of vanadium and oxygen and subsequent thermal processing. This width is approximately an order of magnitude larger than that reported previously for the phase transition of $VO_2$ particles formed in $Al_2O_3$ by a similar technique. The phase transition is accompanied by a significant change in infrared transmission. The anomalously wide hysteresis loop observed here for the $VO_2/SiO_2$ system can be exploited in optical data storage and switching applications in the infrared region. © *2001 American Institute of Physics.* [DOI: 10.1063/1.1415768]

''Smart materials'' have intrinsic properties that combine both sensing and actuating functions. One class of smart materials is based on metal–insulator (or metal–semiconductor) transformations where electrical conductivity changes up to six orders of magnitude occur at a first-order phase transition. The resulting combination of sensing and actuating functions within the same material can be exploited in a wide variety of technological applications that encompass thermochromic coatings,[1] optical[2] and holographic[3] storage systems, fiber-optical switching devices,[4] laser scanners,[5] missile training systems[6] and ultrafast optical switching.[7]

The specific case of the semiconductor-to-metal (S/M) transition observed for vanadium dioxide ($VO_2$) has attracted special attention because its solid-solid structural phase transition at $\sim 68\,^{\circ}C$ is accompanied by a change in its electrical conductivity of almost five orders of magnitude and by associated large changes in its magnetic properties and its optical constants in the technologically critical near-to-midinfrared region. In the present work, we report the formation of a near-surface composite material incorporating micron and smaller-size precipitates of $VO_2$ in an amorphous $SiO_2$ matrix. The S/M phase transition in this material exhibits a hysteresis width greater than $34\,^{\circ}C$, almost an order of magnitude greater than that reported for $VO_2$ precipitates that were created in single-crystal sapphire ($\alpha$-$Al_2O_3$) substrates in previous investigations.[8,9] The unusually reproducible and controllable properties of the material make possible detailed investigations of particle-size effects and host–matrix interactions in the phase transition of $VO_2$.

Since the discovery of the $VO_2$ S/M transition by Morin in 1959,[10] $VO_2$ has been the subject of numerous experimental and theoretical studies. In the first-order[11] phase transition of $VO_2$, the material goes from a tetragonal rutile-structure phase at higher temperature to a monoclinic structure below the phase transition. These structural characteristics led Goodenough[12] to propose a model of the electronic structure based on molecular field theory that has accounted for some properties of the $VO_2$ metallic and semiconducting phases.[13] This model has subsequently undergone further improvements by incorporating electron–electron correlations[14] and electron–phonon interactions. Nevertheless, neither the structural details of the $VO_2$ phase transition nor the dynamics of the transition are completely accounted for.

The $VO_2$/fused–$SiO_2$ near-surface composite in these experiments was formed in a two-step procedure. A room-temperature, stoichiometric coimplantation of vanadium and oxygen was carried out by first implanting V at a fluence of $2\times10^{17}$ V ions/cm$^2$ and energies of 300 or 150 keV. The subsequent oxygen implant was carried out at energies of 120 or 56 keV, respectively, so that, in either case, both the V and O implant profiles overlapped in the same near-surface region of the $SiO_2$ as predicted by TRIM calculations.[15] The implanted $SiO_2$ substrates were then annealed in high-purity flowing argon at temperatures ranging from 800 to $1000\,^{\circ}C$. The $VO_2$ particles produced when the V ions are implanted at 300 keV are found within 500 nm of the top surface of the $SiO_2$ host, with the peak concentration occurring at a depth of 260 nm as measured directly using Rutherford backscattering (RBS) analysis. When the V ions are implanted at 150 keV, the $VO_2$ particles are found within 300 nm of the host surface, i.e., they are closer to, but do not break, the $SiO_2$ surface.

Following the implantation/annealing process, the formation of the $VO_2$ phase was established by x-ray diffraction measurements (XRD) made at the Cu $K\alpha$ wavelength. The presence of the $VO_2$ phase was further confirmed by means of optical transmission measurements using a double-beam spectrophotometer and nonpolarized light. Both types of measurement were performed at different temperatures using a heating stage. Transmission electron microscopy (TEM) as well as RBS studies were carried out in order to determine

[a]Also at Department of Physics and Astronomy, Vanderbilt University; electronic mail: rene.lopez@vanderbilt.edu
[b]Also at: Solid State Division, Oak Ridge National Laboratory.

 

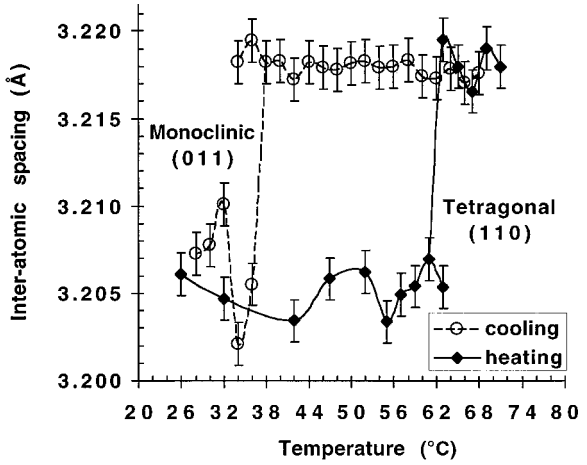


FIG. 1. Enhanced width of the hysteretic phase transition of $VO_2$ precipitates in a fused $SiO_2$ host as illustrated by the variation of atomic $d$ spacings obtained from x-ray diffraction $\theta$–$2\theta$ scans at various temperatures. There is a narrow temperature range at the high and low transition temperatures in which x-ray components from the monoclinic and tetragonal phases coexist. The precipitates were formed by stoichiometrically coimplanting $SiO_2$ with V ($2\times10^{17}$ions/cm$^2$) at 300 keV and with O at 120 keV and thermally annealing in flowing Ar at 1000 °C for 30 min.

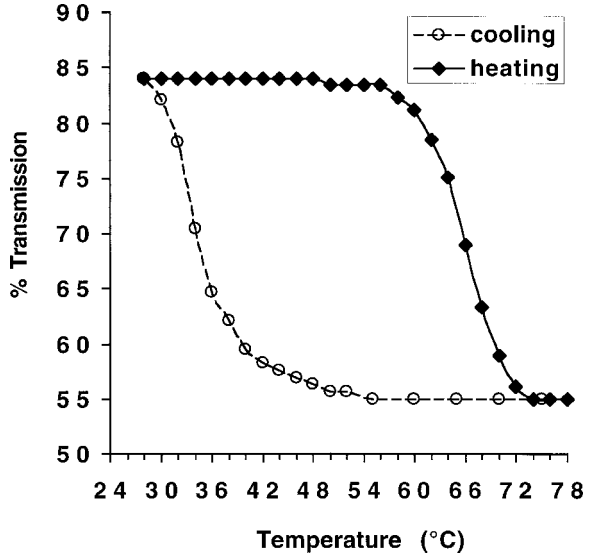


FIG. 2. Temperature dependence of the optical transmission at a fixed wavelength (2 $\mu$m) showing the ~34 °C wide hysteresis loop for $VO_2$ precipitates embedded in fused $SiO_2$. The precipitates were formed by stoichiometrically coimplanting $SiO_2$ with V ($2\times10^{17}$ions/cm$^2$) at 300 keV and with O at 120 keV and thermally annealing in flowing Ar at 1000 °C for 30 min.

the particle size, morphology, and depth distribution of the embedded $VO_2$ precipitates.

The XRD results for a $\theta$–$2\theta$ scan of a fused $SiO_2$ substrate coimplanted with V at 300 keV and with O at 120 keV and annealed at 1000 °C for 30 min show that, in addition to a broad diffuse halo due to the amorphous $SiO_2$ substrate, only a strong Bragg reflection at $2\theta=27.81°$ is observed that is due to the (011) reflection of the monoclinic phase of the embedded $VO_2$ microcrystals. During these $\theta$–$2\theta$ scans, in which the implanted surface lay perpendicular to the scattering vector, no other $VO_2$ reflections appeared in the full range of reflection angles. Thus, we conclude that the assembly of embedded particles, in fact, has a textured, relatively highly oriented structure in spite of the fact that the particles were formed in an amorphous host.

A temperature-dependence study of the observed x-ray reflection is shown in Fig. 1, which presents a plot of the corresponding $d$ spacing versus temperature. Here, it can be seen that, upon heating, the onset of the phase transition, as indicated by the abrupt increase in the $d$ spacing starting from the value characteristic of the monoclinic phase, occurs at ~64 °C. Above 67 °C, the $d$ spacing corresponds to the tetragonal phase of $VO_2$ [using the (110) reflection]. These $d$-spacing values of the precipitates are in good agreement with those measured in standard reference samples[16] [3.202 and 3.220 Å for the (011) monoclinic and (110) tetragonal bulk $VO_2$, respectively]. The temperature onset of the phase transition during the heating cycle is comparable to that found for the best $VO_2$ thin films. In the present case, however, the $VO_2$ particles exhibit a significantly larger undercooling effect resulting in a hysteresis loop whose width spans almost 34 °C. In Fig. 1, the transition from the higher-temperature tetragonal phase to the monoclinic phase upon cooling is indicated by the abrupt decrease in the $d$ spacing shown by the dotted line. The value of ~34 °C for the width of the hysteresis loop is significantly larger than the values that are generally characteristic of standard bulk and thin-film $VO_2$ samples that normally exhibit hysteresis widths of 1–10 °C.[17]

The optical properties of the embedded $VO_2$ particles in fused $SiO_2$ change dramatically in conjunction with the structural phase change corresponding to the x-ray results described above. Figure 2 shows the results of an optical transmission measurement made at a fixed wavelength of 2 $\mu$m as the temperature of the implanted/annealed specimen was scanned at 1 °C/min between 25 and 80 °C. Naturally, these optical transmission results manifest the significantly increased width of the $VO_2/SiO_2$ near-surface-composite hysteresis discussed above. This greater width, and the corresponding effective displacement of the hysteresis loop midpoint closer to room temperature, enhance the potential of the material for optical data storage applications since these features lead directly to an increased and more practical stability range for optically recorded information.

Figure 3 presents a plan-view TEM micrograph of the $VO_2$ precipitates embedded in fused $SiO_2$. The $VO_2$ particles clearly exhibit a broad distribution of sizes, with precipitates ranging from 50 nm to 1 $\mu$m. The largest particles exhibit elongated bar-like shapes, while the smaller precipitates are either slightly oblate or spheroidal. A fraction of the smaller particles also appears to exhibit some evidence of faceting. It has been shown[18] that in general the strain energy per unit volume in those cases where the strain is accommodated by the parent matrix is a function of the spheroidicity of the particles. Accordingly, the observed distribution of shapes among the $VO_2$ precipitates formed here may account for the ~10 °C effective ''roundness'' that is evident in the optical transmission hysteresis loop shown in Fig. 2.

At present there is no clear understanding of the specific mechanism or mechanisms leading to the dramatically increased width of the hysteresis observed here for $VO_2$ precipitates in $SiO_2$, i.e., a hysteresis whose width is about a factor of 10 wider than that for $VO_2$ particles created in

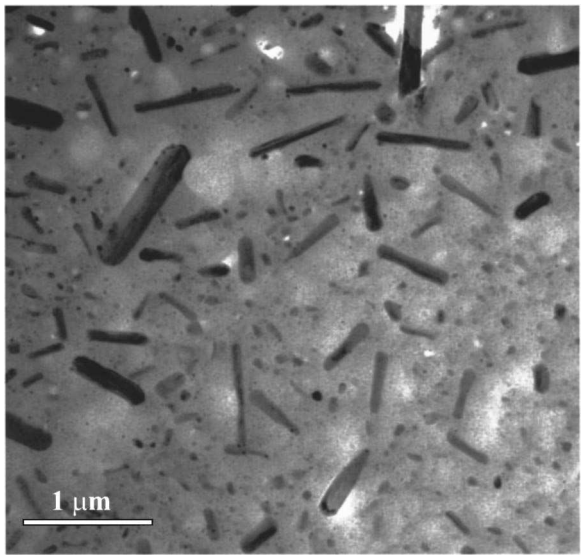


FIG. 3. Transmission electron micrograph of $VO_2$ precipitates in fused $SiO_2$ [coimplanted with V ($2\times10^{17}$ions/cm$^2$) at 300 keV and with O at 120 keV and annealed in Ar at 1000 °C for 30 min]. The micrograph shows the relatively large size distribution of the particles as well as the bar-like shape of the biggest particles and the oblate shape of the smaller precipitates.

(0001)-oriented single-crystal $Al_2O_3$ by a similar process.[9] Our most recent results appear to indicate that the enhanced width is not a consequence of the $VO_2$ precipitate size, since by far the largest volume in the composite is taken up by particles of relatively macroscopic dimensions. Nevertheless, the increased width of the hysteresis points to the existence of additional or larger energetic barriers that retard the phase transition upon cooling in the $VO_2/SiO_2$ system. These barriers may arise from residual stress associated with the annealing step at 1000 °C used to produce the particles. The thermal expansion coefficient of $VO_2$ is $2.1\times10^{-5}$/K,[19] roughly 40 times larger than that of fused silica. Therefore, at room temperature, the $VO_2$ particles in $SiO_2$ will be essentially under tensile stress after the material is cooled to room temperature, and this stress may represent the mechanism responsible for the observed large depression of the temperature at which the metal-to-semiconducting portion of the phase transition occurs upon cooling. In the case of $VO_2$ particles in sapphire, the loop actually exhibits a ''film-like'' width, and in this case, the ratio between the thermal expansion coefficients of $VO_2$ and $Al_2O_3$ is significantly less than in the $VO_2$-particle/$SiO_2$-host case. Experiments are ongoing to determine whether or not effects due to differential thermal expansion are, in fact, responsible for an anomaly of the type observed here.

The present results show that ion implantation and thermal treatments are an effective method by which to create a different type of optically active ''switchable'' surface with unusual characteristics that enhance its applicability in optical switches, self-limiting components, and as an optical storage medium. The results for the $VO_2/SiO_2$ system suggest that the host matrix can play an important role in determining or controlling the properties of near-surface nanocomposite systems. Additionally, detailed investigations of particle-size effects, host–matrix interactions, and dynamical effects on the phase transition of $VO_2$ are now possible due to the capability to form optically and magnetically active precipitates of $VO_2$ in both amorphous and crystalline hosts.

The authors are grateful for the contributions of Karren More and Shawn Trent to the electron microscopy analysis. This research was sponsored by the Laboratory Directed Research and Development Program of Oak Ridge National Laboratory, managed by UT-Battelle, LLC, for the U.S. Department of Energy under Contract No. DE-AC05-00OR22725.

[1] C. G. Granqvist, Phys. Scr. **32**, 401 (1985).
[2] M. Fukuma, S. Zembutsu, and S. Miyazawa, Appl. Opt. **22**, 265 (1983).
[3] W. R. Roach, Appl. Phys. Lett. **19**, 453 (1971).
[4] C. E. Lee, R. A. Atkins, W. N. Giler, and H. F. Taylor, Appl. Opt. **28**, 4511 (1989).
[5] J. S. Chivian, W. E. Case, and D. H. Rester, IEEE J. Quantum Electron. **QE-15**, 1326 (1979).
[6] M. A. Richardson and J. A. Coath, Opt. Laser Technol. **30**, 137 (1998).
[7] M. F. Becker, A. B. Buckman, R. M. Wasler, T. Lepine, and P. Georges, Proc. SPIE **2189**, 400 (1994).
[8] L. A. Gea and L. A. Boatner, Appl. Phys. Lett. **68**, 3081 (1996).
[9] L. A. Gea, J. D. Budai, and L. A. Boatner, J. Mater. Res. **14**, 2602 (1999).
[10] F. J. Morin, Phys. Rev. Lett. **3**, 34 (1959).
[11] *Vibrational Spectroscopy of Phase Transitions*, edited by Z. Iqbal and F. J. Owens (Academic, Orlando, FL, 1984).
[12] J. B. Goodenough, J. Solid State Chem. **3**, 490 (1971).
[13] S. Shin, S. Suga, M. Taniguchi, M. Fijisawa, H. Kansaki, A. Fujimori, H. Damon, Y. Ueda, K. Kosuge, and S. Kachi, Phys. Rev. B **41**, 4993 (1990).
[14] D. Paquet and P. Leroux-Hugon, Phys. Rev. B **22**, 5284 (1980).
[15] J. F. Ziegler, Transport and Range of Ions in Matter, Ver. 96.01, IBM Research, Yorktown Heights, NY, 1996.
[16] D. Kucharezyk and T. Niklewski, J. Appl. Crystallogr. **12**, 370 (1979).
[17] J. F. DeNatale, P. J. Hood, and A. B. Harker, J. Appl. Phys. **66**, 5844 (1989).
[18] F. R. N. Nabarro, Proc. R. Soc. London, Ser. A **175**, 519 (1940).
[19] M. Guntersdorfer, Solid-State Electron. **13**, 355 (1970).